

A Novel Algorithm for Community Detection in Networks using Rough Sets and Consensus Clustering

Darian H. Grass-Boada^{a,b,*}, Leandro González-Montesino^{a,b}, Rubén Armañanzas^{a,b}

^a*Institute of Data Science and Artificial Intelligence (DATAI), Campus Universitario, Edificio Ismael Sánchez Bella, Pamplona, 31009, Navarra, Spain*

^b*TECNUN School of Engineering, Manuel Lardizabal Ibilbidea, 13, Donostia-San Sebastián, Gipuzkoa, 20018, País Vasco, Spain*

Abstract

Complex networks, such as those in social, biological, and technological systems, often present challenges to the task of community detection. Our research introduces a novel rough clustering-based consensus community framework (RC-CCD) for effective structure identification of network communities. The RC-CCD method employs rough set theory to handle uncertainties within data and utilizes a consensus clustering approach to aggregate multiple clustering results, enhancing the reliability and accuracy of community detection. This integration allows the RC-CCD to effectively manage overlapping communities, which are often present in complex networks.

This approach excels at detecting overlapping communities, offering a detailed and accurate representation of network structures. Comprehensive testing on benchmark networks generated by the Lancichinetti–Fortunato–Radicchi method showcased the strength and adaptability of the new proposal to varying node degrees and community sizes. Cross-

*Correspondence to: dhgrass@unav.es (D.H. Grass-Boada)

comparisons of RC-CCD versus other well-known detection algorithms out-comes highlighted its stability and adaptability.

Keywords: community detection, complex networks, rough set theory, graph theory

1. Introduction

Identifying community structures in complex networks, commonly known as community detection [1], is prevalent in fields like social analysis[2, 3], life sciences [4], and computational systems [5]. The identification of closely linked nodes, clusters of common structures, and information flows is key to understand the organizational and functional dynamics of a network system. Algorithms for finding these communities benefit from the modular nature of real-world networks, characterized by larger intra-community relationships than inter-community links [6].

We introduce here a novel community detection method for complex networks named rough clustering-based consensus community framework (RC-CCD) that integrates rough set theory [7] and consensus clustering. Distinguishing itself from Lancichinetti et al.’s matrix-based approaches [8], our algorithm accurately identifies overlapping communities, leveraging lower and upper rough set approximations and a thresholded similarity graph. This novel method provides a more nuanced analysis of network structures, especially in intricate systems like social and biological networks.

The effectiveness of the new algorithm was rigorously tested using synthetic networks produced by the Lancichinetti–Fortunato–Radicchi (LFR) benchmark generator [9]. The RC-CCD demonstrated superior performance

in terms of normalized mutual information compared to established community detection algorithms such as the Louvain, Greedy and LPA. Our comprehensive evaluation involved varying network scales and complexities, highlighting RC-CCD’s robust adaptability and consistently higher accuracy in detecting nuanced community structures across diverse network topologies.

The paper is structured as follows: Section 2 describes the related work on community detection algorithms. Section 3 explains our methodology. Section 4 presents experimental results and comparisons with traditional algorithms. Section 6 concludes and suggests future research directions.

2. Related Work

Existing community detection algorithms often fall short in accurately detecting said communities due to the unique characteristics of each network. This variation underlines the need for more sophisticated methods to refine detection accuracy. Addressing these challenges, consensus clustering, as highlighted by Lancichinetti et al. [8] and Jeub et al. [10], has marked a significant advancement, merging multiple clustering results into a unified representation and reducing algorithmic randomness and biases.

One noteworthy example is the dual-level clustering ensemble algorithm [11], which incorporates a comprehensive approach using three consensus strategies to generate a highly consistent outcome. Each type addresses the information from base clustering members differently, contributing uniquely to the production of the ensemble outcome.

Another example of the application of ensemble clustering in the discov-

ery of cancer subtypes is the work by Parea et al. [12], where a multi-view hierarchical ensemble clustering approach showed excellent performance in stratifying patients into sub-groups. The groups successfully mapped similar molecular characteristics across several types of cancer, outperforming current state-of-the-art methods in six out of seven cancer types. More innovative methods continue to emerge, aiming to refine clustering performance through ensemble and consensus strategies. Ji et al. [13] introduced a clustering ensemble algorithm optimizing the accuracy of equivalence granularity to improve clustering quality by minimizing input data size and enhancing the diversity and accuracy of the base groupings.

The exploration of consensus clustering in complex networks has significantly advanced our understanding of network structures. Lancichinetti and Fortunato [8] were pioneers in demonstrating the efficacy of consensus clustering for enhancing the stability and accuracy of community detection in complex networks. Their methodology set a foundation for subsequent research by addressing the limitations inherent in single-resolution community detection methods. Inspired by this foundational work, Jeub et al. [10] introduced the concept of multiresolution consensus clustering. This approach not only acknowledges the multi-scale nature of community structures within networks, but also provides a framework for identifying these structures across different resolutions. Their methodology emphasizes the benefits of hierarchical consensus clustering on networks that exhibit complex, layered community structures. Further advancements in the field were made by Tandon et al. [14], who developed a fast consensus clustering technique that significantly reduces the computational demand of the consensus clustering

process. This innovation enabled the application of consensus clustering to much larger networks than was previously feasible, marking a significant step forward in network analysis capabilities.

These contributions collectively highlight the evolving landscape of consensus clustering research, demonstrating its critical role in uncovering the nuanced community dynamics of complex networks. Building upon these significant contributions, our work overcomes prior limitations by integrating rough set theory with consensus clustering in the context of community detection in networks. By incorporating the rough set framework, our method is capable of accurately identify overlapping communities beyond the reach of previous matrix-based methods. This integration not only differentiates our method from the matrix-based strategies employed by Lancichinetti et al. [8] but also addresses the critical challenge of detecting overlapping communities with high accuracy. Leveraging the principles of lower and upper rough set approximations in conjunction with a thresholded similarity graph, our algorithm offers a more nuanced and sophisticated analysis, enabling a deeper exploration of the dynamics of a complex network.

3. Rough Clustering-Based Consensus Community Detection (RC-CCD)

3.1. Networks as graphs

A network is represented as a graph $G = (V, E)$, where V denotes the set of nodes and E the set of edges connecting these nodes. The graph G is characterized by an adjacency matrix A , with elements A_{ij} representing the presence (1) or absence (0) of an edge (v_i, v_j) between nodes i and j . The

degree of a node v_i , denoted by d_{v_i} , represents the number of edges pointing to node v_i .

Communities or clusters within a network are identified as subgraphs with high internal edge density while their external edge density is low. Formally, a community structure is a division $\mathbb{P} = \{C_1, C_2, \dots, C_k\}$ of the network into k subgraphs, where $V = \bigcup_{i=1}^k C_i$.

Definition 1 (Thresholded similarity graph). *Given a set of nodes $V = \{v_1, v_2, \dots, v_n\}$ of a network G , and a threshold β , the thresholded similarity graph G_β is an undirected graph where an edge (v_i, v_j) exists if the similarity between nodes v_i and v_j is at least β .*

Definition 2 (Subgraph). *A graph G_1 is a subgraph of G_2 , denoted as $G_1 \subseteq G_2$, if every vertex and edge in G_1 is also in G_2 .*

Definition 3 (Induced Subgraph). *For a graph G and a vertex subset $V' \subseteq V$, the induced subgraph $G[V']$ is composed of V' and all edges in G that connect pairs of nodes in V' .*

Definition 4 (β -Connected Component). *In a thresholded similarity graph G_β , a subgraph G' is a β -connected component if every pair of distinct nodes in G' is connected directly or indirectly, and there is no larger subgraph containing G' that also satisfies this condition.*

3.2. RC-CCD Algorithm

Our proposal combines Rough Set Theory (RST) [7, 15] with the rough k -means algorithm [16] for a nuanced analysis of network structures. Initially, we identify similar node sets within the network G , leading to a partition of V

and establishing node equivalences based on their co-location in communities. This step not only groups nodes but it also provides inter-node relationships key to accurately set the final communities.

In the second phase, network communities are treated as rough sets, revealing overlapped groups for a more realistic representation of the network’s structure, illustrating the connections and shared elements among communities. This augmentation is designed to provide a clearer understanding of complex community structures in the network [17].

3.2.1. First step: build the granules of indiscernible nodes

The initial phase of our approach involves creating a thresholded similarity graph, which captures the relationships between network nodes. This is achieved by analyzing the frequency of nodes jointly included in communities produced by different algorithms.

Nodes similarity measure. Let $\mathbb{NP} = \{\mathbb{P}_1, \mathbb{P}_2, \dots, \mathbb{P}_p\}$ a set of network partitions of G , comprising partitions from various runs of different algorithms used for consensus. Notably, each algorithm is expected to produce distinct partitions based on a variety of mathematical foundations. Here, \mathbb{P}_r represents an individual partition within \mathbb{NP} for $1 \leq r \leq p$, where p equals the total number of runs across all algorithms.

We define the similarity function $S_{\mathbb{NP}}(v_i, v_j)$ to measure the closeness of nodes v_i and v_j based on their co-occurrence across \mathbb{NP} . This function quantifies the degree of association between two nodes within the context of the given network partitions.

Let \mathbb{CS}_{v_i} be the set of communities where vertex v_i is included. We define

$mc(v_i, v_j)$ as the count of common communities between nodes v_i and v_j , within the partition \mathbb{P}_r . This definition is a formalization of the elements i, j of the consensus matrix D from the work of Lancichinetti et al [8]. The similarity function $S_{\mathbb{NP}}(v_i, v_j)$ is then defined as:

$$S_{\mathbb{NP}}(v_i, v_j) = \frac{\sum_{\mathbb{P} \in \mathbb{NP}} match(v_i, v_j)}{|\mathbb{NP}|}, \quad (1)$$

where $match(v_i, v_j)$ is calculated by:

$$match(v_i, v_j) = \frac{mc(v_i, v_j)}{|\mathbb{CS}_{v_i}| \cdot |\mathbb{CS}_{v_j}|}. \quad (2)$$

Indiscernible nodes granules. The thresholded similarity graph G_β is constructed using a similarity measure $S_{\mathbb{NP}}(v_i, v_j)$ and a user-defined threshold β within $[0, 1]$. In G_β , edges represent the frequency with which nodes v_i and v_j co-occur in the same communities across the set of network partitions \mathbb{NP} . Connected components derived from G_β , denoted by $G'_r = \{G'_{r_1}, G'_{r_2}, \dots, G'_{r_q}\}$, highlight groups of nodes with strong community ties, that is the granules from the network's modular structure.

The method focuses on identifying sets of indiscernible nodes within the graph G . These nodes are termed indiscernible because they exhibit identical characteristics or connectivity patterns according to the criteria established by the algorithm, making them indistinguishable within the network context. The process identifies these sets and constructs induced subgraphs from them, which are denoted collectively as G'_r . Each subgraph represents a cluster of nodes that share strong similarities, and these clusters are crucial in forming the granular set $G_r = \{G_{r_1}, G_{r_2}, \dots, G_{r_q}\}$.

Each subgraph in G_r corresponds to a group of nodes that share similar characteristics or roles within the network, effectively partitioning the

vertex set V . This partitioning establishes equivalence relations among the nodes. An equivalence relation in this context implies that any two nodes connected by this relation are considered equivalent under the criteria set by the method, primarily based on their shared community memberships in \mathbb{NP} . This mechanism helps in understanding the structure of the network by clustering nodes that are similar, thus simplifying the complexity of the network’s overall analysis.

3.2.2. Second step: build the final covering of G

The second phase applies the rough k -means algorithm [16] to refine network coverage. This step is specifically designed to identify overlapping communities. We select k community prototypes from G_r (where $1 \leq k \leq q$) based on vertex count, integrating the remaining granules to effectively depict the network’s complexity. This phase leverages lower and upper approximations to provide a comprehensive representation of community structures.

Selection of k prototypes. Our method selects k core prototypes for consensus communities based on input from various baseline algorithms to form a collection \mathbb{NP} , each yielding partitions \mathbb{P}_r with k_r communities. These algorithms often identify larger communities first, influencing the selection process. We choose k based on the number of communities covering the most network nodes, ensuring that these prototypes represent significant network areas.

A cumulative frequency histogram is created from these partitions, merging bars representing the same k_r -th community. The histograms are ordered by frequency, and k is determined by the count of the top histograms cover-

ing 90% of the total frequency. The top k communities are then selected as prototypes for our consensus clustering.

Assign the remaining granules. After the initial k prototype selection, our method efficiently assigns the remaining granules to these cores, using two defined similarity functions for precise community delineation between any two granules $G_{r_i}, G_{r_j} \in G_r$. At this stage, G_{r_i} represents the i -th prototype (where $1 \leq i \leq k$), and G_{r_j} denotes the j -th remaining granule to be assigned (where $k + 1 \leq j \leq q$).

The first similarity function $S_{G_r}(G_{r_i}, G_{r_j})$ measures granule similarity by assessing vertex co-location in the same community across partitions in \mathbb{NP} :

$$S_{G_r}(G_{r_i}, G_{r_j}) = \sum_{v_i \in G_{r_i}} \sum_{v_j \in G_{r_j}} S_{\mathbb{NP}}(v_i, v_j) \quad (3)$$

where, $S_{\mathbb{NP}}(v_i, v_j)$ is the nodes similarity measure defined in Equation 1.

The second function, $S_{E_r}(G_{r_i}, G_{r_j})$, quantifies the connections between nodes within granules:

$$S_{E_r}(G_{r_i}, G_{r_j}) = \sum_{v_i \in G_{r_i}} \sum_{v_j \in G_{r_j}} A_{v_i, v_j} \quad (4)$$

For each prototype G_{r_i} , we compute $S_{G_r}(G_{r_i}, G_{r_j})$ for all j -th granules and normalize these values within $[0, 1]$ using the maximum S_{G_r} , denoted as $S_{G_r}^{max}$. A similar normalization is applied to E_{G_r} , yielding normalized values with respect to $E_{G_r}^{max}$. We then derive a composite metric, $CS_{G_{r_j}}$, as the average of these normalized values for each granule G_{r_j} .

$$CS_{G_{r_j}} = \frac{1}{2} \left(\frac{S_{G_r}(G_{r_i}, G_{r_j})}{S_{G_r}^{max}} + \frac{E_{G_r}(G_{r_i}, G_{r_j})}{E_{G_r}^{max}} \right) \quad (5)$$

Each granule G_{r_j} is assigned to community approximations based on its score $CS_{G_{r_j}}$ and a threshold γ within $[0, 1]$. Granules exceeding γ in similarity to a prototype G_{r_i} join the lower approximation, indicating strong alignment, while others enter the upper approximation for weaker associations. This method effectively delineates community structures, capturing both clear and ambiguous node relationships in the network.

The *Rough Clustering-Based Consensus Community Detection Algorithm* (RC-CCD), outlined in Algorithm 1 (code available at ¹), begins by selecting k community prototypes from baseline algorithms as initial lower approximations. Subsequent granules are assigned to either lower or upper approximations based on their similarity scores, $CS_{G_{r_j}}$.

RC-CCD integrates Rough Set Theory with community detection to identify both distinct and ambiguous network structures, excelling in detecting overlapping communities. Our method innovatively adapts the β -thresholded graph and consensus matrix approach from Lancichinetti et al. [8], enhancing community detection accuracy by analyzing connection strengths within and around communities. RC-CCD represents a significant leap in community detection, effectively handling complex network structures with methodological precision.

¹<https://github.com/Leandroglez39/RoughSetsConsensusClustering>

Algorithm 1: Rough Clustering-Based Consensus Community Detection algorithm pseudo-code.

Input: Network $G = (V, E)$, Set of Network Partitions \mathbb{NP}

Output: Consensus-Based Network Coverage

$$CV = \{CV_1, CV_2, \dots, CV_k\}$$

Step 1: Build Granules of Indiscernible Objects;

for each pair of nodes $v_i, v_j \in V$ **do**

 | Compute similarity $S_{np}(v_i, v_j)$ using \mathbb{NP} and β parameter;

end

Construct thresholded similarity graph G_β ;

Identify β -connected components in G_β ;

Form granules set $G_r = \{G_{r_1}, G_{r_2}, \dots, G_{r_q}\}$;

Step 2: Build Final Network Coverage;

Sort G_r in descending order of vertex count;

Select top k granules as prototypes for communities CV_i ;

for $i \leftarrow 1$ to k **do**

 | Assign G_{r_i} to CV_i ;

end

for $j \leftarrow k + 1$ to q **do**

 | Assign G_{r_j} to lower \underline{CV}_i or upper \overline{CV}_i approximations based on
 | composite similarity and γ parameter;

end

return CV ;

4. Experimental Setup

4.1. Base Algorithms & Metrics

In this work, we used four state-of-the-art community detection algorithms as both inputs and also benchmarks to test our RC-CCD method [18, 19, 20, 21]. A brief description of each algorithm follows:

- **Louvain** is a hierarchical clustering algorithm with a complexity of $\mathcal{O}(V \cdot \log V)$. Effective at optimizing network modularity and identifying diverse community sizes, it may struggle with small communities in the presence of larger ones. It converges when modularity cannot be further improved [18].
- **Greedy Modularity** is an agglomerative algorithm similarly focused on optimizing modularity, with a computational complexity of $\mathcal{O}(E \cdot \log^2 V)$. While effective, its computational demand makes it less suitable for large networks and it faces challenges in detecting smaller communities. Convergence occurs when no community fusion increases modularity [19].
- **Label Propagation (LPA)** is a non-deterministic algorithm with a linear complexity of $\mathcal{O}(E)$. LPA tends to identify balanced-sized communities but may overlook smaller ones in dense networks. It stabilizes when a node’s label matches the majority of its neighbors’ [20].
- **Infomap** uses information theory with efficient time performance, capable of detecting various community sizes, including nested and overlapping ones. It might yield very small communities and stabilizes when the description length of the random walk is minimized [21].

Two well-known graph metrics were used to assess performance and compare the output communities across runs of each algorithm.

Normalized Mutual Information (NMI) is a commonly used metric in the field of network analysis and community detection [22]. It serves to evaluate the performance of community detection algorithms by measuring the similarity between two different community assignments. Specifically, it compares a ground truth community structure with the outcome community structure from an algorithm, taking into account both the homogeneity and completeness of the assignments.

The NMI value lies in the range of 0 to 1. A value of 1 signifies a perfect match, while a value of 0 indicates no similarity between the two community assignments. A higher NMI value thus implies a stronger agreement between the community structures under comparison, serving as a quantitative measure for evaluation and comparison of different methods.

Participation Coefficient (PC) is another well-used metric in the community detection field [23]. It quantifies the diversity of a node’s connections across different communities in a network. The PC for a node v_i is given by:

$$P(v_i) = 1 - \sum_{s=1}^k \left(\frac{d_{v_i,s}}{d_{v_i}} \right)^2 \quad (6)$$

Here $d_{v_i,s}$ represents the number of links from node v_i to nodes in community s , d_{v_i} is the node’s total degree, and k is the total number of communities. To extend the applicability of the PC to networks with overlapping communities, the total degree d_{v_i} of a node is modified as follows:

$$d_{v_i} = \sum_{c \in C} h_{v_i, c} \quad (7)$$

where C represents the set of communities and $h_{v_i, c}$ is the count of node i 's neighbors that also belong to community c .

4.2. Synthetic Networks

Our study uses the *LFR* framework to generate test networks of various power-law distributions in vertex degree and community size, reflecting real-world network characteristics [9]. The *LFR* framework can accurately replicate complex network structures while providing the truth communities for comparison. Key parameters when generating the networks include node degrees and community sizes, governed by τ_1 and τ_2 , as well as network size N , average degree k , maximum degree k_{\max} , and community size range limits c_{\min} and c_{\max} . A key feature of *LFR* is the mixing parameter μ that controls the fraction of inter-community edges, with lower values yielding clearer clusters and higher values resulting in mixed communities. For those networks with overlapping communities, two other parameters are also key: O_n as the overlap rate, and O_m as the node participation in multiple communities.

In our experiments, we configured two distinct sets of parameters to assess the influence of network size on community detection. We varied μ from 0.1 to 0.6 in increments of 0.05, generating 11 distinct networks for each configuration, labeled from *net1* to *net11*. These labels will be consistently used in subsequent tables and figures to denote the specific networks analyzed. The full configurations for the two types of networks were as follows:

- Small network configuration: $n = 1000$, $\tau_1 = 2$, $\tau_2 = 1$, $k = 15$,
 $k_{\max} = 50$, $c_{\min} = 20$, $c_{\max} = 50$, $O_n = 100$, $O_m = 2$
- Large network configuration: $n = 20000$, $\tau_1 = 2$, $\tau_2 = 1$, $k = 15$,
 $k_{\max} = 50$, $c_{\min} = 40$, $c_{\max} = 100$, $O_n = 2000$, $O_m = 2$

5. Results

This section provides a comprehensive evaluation and comparison of the RC-CCD algorithm and the baseline algorithms from Section 4.1. The evaluation of RC-CCD included NMI for accuracy, analysis of variability in community detection or outcome stability, a modified participation coefficient for overlapping communities, and an analysis of community structures at different scales for boundary detection. All these evaluations were carried on over *LFR*-generated synthetic networks. With respect to RC-CCD’s parameters β and γ , we set $\beta = 0.75$ and $\gamma = 0.8$, as indicated elsewhere [24, 16, 25].

5.1. NMI quality measure

We firstly assessed and compared the accuracy of the RC-CCD and the baseline algorithms’ outcomes based on the NMI metric (see 4.1), including small ($n = 1000$) and large networks ($n = 20000$). A visual summary of the NMI scores across algorithms is shown in Figure 1. Extended NMI results are included Tables A.5 and A.6 in the *Supplementary Material*.

For small networks, RC-CCD consistently achieves high NMI values, often above 0.85, indicating strong alignment with ground-truth communities. While baseline algorithms Infomap and Louvain show robust performance, LPA notably scores an NMI of zero in *net10* ($\mu = 0.55$) and *net11* ($\mu = 0.6$),

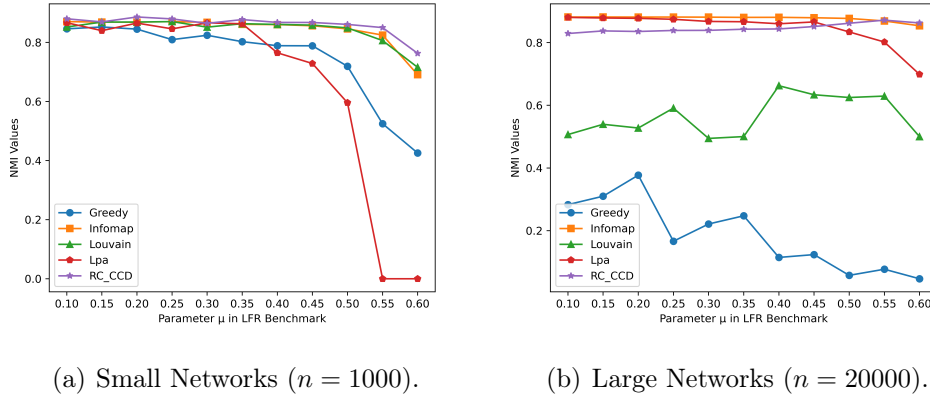


Figure 1: Comparison of the baseline algorithms and RC-CCD on *LFR* benchmark.

suggesting a complete mismatch with the actual community structure. The Greedy algorithm generally under performs across all runs.

For large networks, RC-CCD consistently achieves results that are equal to or better than the other evaluated algorithms. For example, in *net1*, the NMI score of 0.829 for RC-CCD is close to Infomap’s 0.882 and significantly higher than Greedy’s 0.283. Notably, in more complex networks such as *net10* and *net11*, RC-CCD achieves slightly higher values than Infomap, which consistently maintains high scores across networks. In contrast, the Greedy algorithm continues to perform poorly, maintaining low values throughout.

In summary, RC-CCD demonstrates reliable and accurate community detection in diverse networks, as evidenced by consistent high NMI scores (see Tables A.5 and A.6). Its robustness and adaptability are further validated through comprehensive comparisons with baseline algorithms, as shown in Figure 1.

5.2. Stability

Stability, essential for measuring algorithm consistency across multiple runs [26], was quantitatively assessed using the NMI index to track community assignment consistency by all the algorithms.

Small and large network configurations were tested through 10, 50, and 100 runs, each replicated $r = 20$ times, to confirm result consistency. Mean NMI scores from these repetitions served as indicators of stability, with the modularity metric used to identify distinct community structures from multiple algorithm outputs.

Summarized in Table 1 and 2, the evaluation on complex networks ($\mu = 0.6$) showed that in small configurations, LPA was unstable with zero NMI (Table 1). Greedy averaged 0.43 ± 0.05 in NMI, while Louvain and Infomap showed moderate stability with 0.71 ± 0.03 and 0.67 ± 0.04 respectively. RC-CCD demonstrated superior stability with an average NMI of 0.76 ± 0.01 .

Alg	$\mu = 0.6$		
	10	50	100
LPA	0.00 ± 0.00	0.00 ± 0.00	0.00 ± 0.00
Greedy	0.43 ± 0.05	0.41 ± 0.05	0.43 ± 0.04
Louvain	0.71 ± 0.03	0.70 ± 0.03	0.70 ± 0.03
Infomap	0.67 ± 0.04	0.66 ± 0.06	0.68 ± 0.07
RC-CCD	0.76 ± 0.01	0.73 ± 0.01	0.76 ± 0.00

Table 1: Small Network Configuration: NMI quality and standard deviation comparison of RC-CCD and baseline algorithms for network complexity $\mu = 0.6$

In larger networks, RC-CCD maintained high stability with NMI scores between 0.86 and 0.87 (see Table 2). Infomap slightly decreased to around

0.85 NMI, while Louvain improved to 0.63-0.64 NMI. LPA showed significant improvement from its small network instability, achieving NMI values in the 0.69-0.71 range. Conversely, the performance for the Greedy alternative dropped to a low of 0.03 NMI.

	$\mu = 0.6$		
Alg	10	50	100
LPA	0.71 ± 0.00	0.71 ± 0.00	0.69 ± 0.00
Greedy	0.03 ± 0.00	0.03 ± 0.00	0.03 ± 0.00
Louvain	0.63 ± 0.00	0.64 ± 0.00	0.62 ± 0.00
Infomap	0.85 ± 0.00	0.85 ± 0.00	0.85 ± 0.00
RC-CCD	0.86 ± 0.00	0.86 ± 0.00	0.87 ± 0.00

Table 2: Large Network Configuration: NMI quality and standard deviation comparison of RC-CCD and baseline algorithms for network complexity $\mu = 0.6$

Notably, LPA performance shifted from unstable ranges in small networks to moderate stability in larger ones, while RC-CCD and Infomap maintained high values across network sizes, showcasing their robustness. Detailed stability summaries are detailed in Supplementary Material Table B.7 and Table B.8. An interesting observation across all algorithms was the absence of standard deviation in the NMI scores, indicating a highly consistent performance within each method across multiple runs. These stability results also highlighted the impact of network complexity (μ) on the algorithms performance. Even with these varying network complexities, RC-CCD emerged as a highly reliable and adaptable choice.

5.3. Cores Accuracy Evaluation

Our research enhances classical community detection approaches by using a lower approximation to find the core elements of each community from the k communities determined by multiple algorithm runs. The accuracy in finding these cores when compared to the ground-truth distribution (GT) for both small and large networks is presented in Table 3.

Nets	net1	net2	net3	net4	net5	net6	net7	net8	net9	net10	net11
Small	93.7	93.9	92.6	94.7	93.4	93.8	93.3	90.0	89.7	96.5	96.1
Large	92.8	95.5	94.9	95.2	94.2	95.0	93.2	93.8	91.7	90.6	83.6

Table 3: Accuracy of RC-CCD’s lower approximation when finding ground-truth communities in small and large networks

The results across small and large network configurations revealed that the proposed method for determining lower approximations consistently reached accuracy values over 90%. The evaluation in Table 3 also showed that the method is consistent across varying degrees of network complexity.

The analysis of the number of communities k identified by the RC-CCD method is pivotal. In Table C.9 within the Supplementary Material, we compare the counts of communities detected by RC-CCD to those of the GT. This comparison across 11 networks with varied complexities highlights the accuracy of our method in identifying community structures. The results show clear trends in how the complexity of the network influences the precision of the community detection by RC-CCD.

In small networks, our approach matched the GT for community number (k) across networks net1 to net9 ($k = 31$), showcasing its strength in accu-

rately identifying community structures in less connected environments. For larger networks, the method showed enhanced precision in complex settings, especially in *net10* and *net11* where it closely approximated the GT. The RC-CCD method demonstrated outstanding performance on the network *net11*, identifying $k = 366$ communities, compared to $k = 337$ communities detected by the GT. This result underscores the adaptability and efficiency of RC-CCD in handling networks of larger and more complex structures.

5.4. Evaluation of Community Overlap

Although our algorithm was not explicitly designed to identify overlapping communities, its mathematical formulation allows for it. This represents a significant advancement beyond previous studies [8, 10], as it identifies nodes that can belong to multiple communities. In our experiments, we configured the *LFR* benchmark engine with a 10% overlapping rate to evaluate RC-CCD’s performance in this task. Participation Coefficient (PC) was used to assess the degree of a node’s involvement across different communities. We compared the nodes included in the overlapping communities identified by our method with those in the overlapping communities from the ground-truth. Higher PC values indicate that a node is active in multiple communities, and our results confirmed that RC-CCD effectively identifies these overlapping nodes.

Table 4 presents the average PC degree for both ground truth and RC-CCD results across networks of varying complexities (μ), for both small ($n = 1000$) and large ($n = 20000$) networks. These values progressively increased with network complexity, reflecting RC-CCD improved detection of overlapping communities as the network becomes more intricate.

Net	PC_Mean_GT		PC_Mean_RC		T_Positive		F_Positive	
	Small	Large	Small	Large	Small	Large	Small	Large
net1	0.65	0.66	0.61	0.64	9	208	0	36
net2	0.70	0.70	0.69	0.66	3	221	0	0
net3	0.73	0.73	0.68	0.73	16	189	0	102
net4	0.75	0.75	0.70	0.76	10	124	0	77
net5	0.77	0.78	0.76	0.79	11	167	0	0
net6	0.80	0.80	0.78	0.81	13	195	0	36
net7	0.82	0.82	0.81	0.82	8	204	2	40
net8	0.84	0.84	0.81	0.84	10	215	0	4
net9	0.85	0.86	0.82	0.84	16	231	1	47
net10	0.88	0.88	0.84	0.86	14	216	6	21
net11	0.88	0.89	0.85	0.87	20	256	16	87

Table 4: Comparative Analysis of mean Participation Coefficient values and True/False Positives for RC-CCD Against ground-truth communities in small and large networks.

For smaller networks, the RC-CCD method’s PC values were slightly lower (e.g., 0.61 for RC-CCD versus 0.65 for GT in *net1*) than in more complex networks (e.g., 0.85 for RC-CCD versus 0.88 for GT in *net11*). A similar trend was observed in larger networks, where initial PC values were marginally lower for RC-CCD but approach ground truth values as network complexity increased (e.g., from 0.64 for RC versus 0.66 for GT in *net1*, to 0.87 for RC-CCD versus 0.89 for GT in *net11*).

Additionally, we conducted a thorough comparison of our method’s performance in detecting overlapping nodes against the ground truth, across different network sizes. This analysis, detailed in Table 4, included assessments of both true and false positive rates. In smaller networks like *net1*, our method showed precision by identifying 9 out of 100 overlapping nodes with no false positives. Notably, for small networks, zero false positives were recorded in networks *net2*, *net3*, *net4*, *net5*, and *net8*, demonstrating good accuracy across a spectrum of complexities. This result confirmed that the detected overlaps by RC-CCD were indeed accurate, even though it captured a modest number of true positives. Conversely, in larger networks like *net11*, there was a significant increase in true positive detection –256 out of 2000 nodes– along with an increase in false positives to 87.

Figure 2 further illustrates these findings for networks with a complexity of $\mu = 0.6$ (*net11*), covering both small and large network sizes. In large networks, nodes identified as overlapping generally showed higher PC values, whereas smaller networks exhibited a more compact distribution of PC values, reflecting the RC-CCD method’s precision in simpler network contexts.

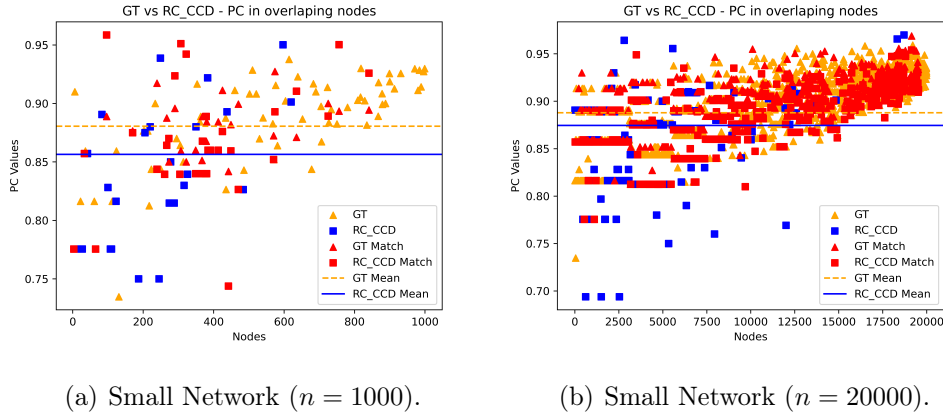


Figure 2: Comparison of Participation Coefficient values for overlapping nodes identified by RC-CCD and ground-truth communities overlapping nodes on the *LFR* benchmark.

5.5. Boundary Structure Under Different Upper Approximation Scales

The γ parameter in our RC-CCD method introduces a level of adaptability, allowing for the fine-tuning of overlapping vertex detection across various network structures. By adjusting this parameter, we will have boundaries of communities more or less tight. In the above experiments, we set the parameter $\gamma = 0.8$ as a basic level for detecting community structures. To understand how RC-CCD adapts to changes in γ , we studied three other values, namely 0.5, 0.6, and 0.7, keeping β constant. γ acts as a tuning parameter with higher values expanding boundaries, and lower values contracting them.

The effects of varying γ on RC-CCD effectiveness are detailed in Supplementary Tables D.10 and D.11 showing results for NMI in small and large networks, respectively. Figure 3 illustrates two examples using the NMI metric in which RC-CCD outperforms all baseline algorithms under different γ values (refer to Supplementary Table D.10 and D.11 for numeric values).

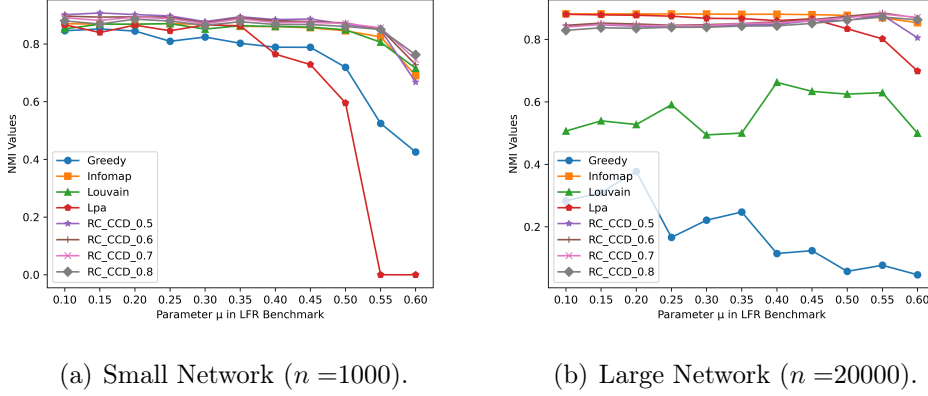


Figure 3: Comparison of baseline algorithms and RC-CCD (with varying γ settings) outcomes on the *LFR* benchmark.

Our findings highlight the RC-CCD method’s ability to adjust to network complexities via strategic γ parameter tuning. In simpler networks, like *net1*, a γ setting of 0.5 yielded an optimal NMI score of 0.902, illustrating the advantage of expanding community boundaries in less complex structures. Conversely, in the most intricate network, *net11*, a higher γ of 0.8 produced the best NMI score of 0.763. This trend is consistent across large networks, where less complex networks achieve higher NMI scores with lower γ values, and the most complex networks reached peak NMI scores with large γ values. Tables D.10 and D.11 corroborate this trend.

In addition to the NMI comparison, Tables E.12 and E.13 present results for Participation Coefficient, for both true and false positives in small and large networks, respectively. RC-CCD performed well when changing the γ values. Note that the results for small networks tended to minimize false positives (FP) across networks of low to medium complexity under var-

ious γ values. For networks *net1* through *net7* specifically, our approach consistently reported zero false positives across all γ settings (0.5, 0.6, and 0.7), accurately identifying true positives (TP) without misclassifying non-membership nodes in simpler networks. In the case of larger networks, the results demonstrate that both true positives and false positives increased with the variation of gamma, being more noticeable with $\gamma = 0.5$. Overall, RC-CCD proved to be highly effective at identifying overlapping nodes accurately with minimal false positives.

6. Discussion

This work introduces RC-CCD, a novel consensus clustering approach that effectively combines multiple community detection algorithms to enhance precision and adaptability in identifying network community structures. By integrating results from different methodologies, RC-CCD addresses inherent limitations of single-algorithm approaches and leverages collective strengths, providing a more resilient and versatile solution.

The performance evaluation of RC-CCD using the NMI metric showed a high accuracy in discovering ground-truth communities, as well as demonstrating good performance despite the size of the networks. RC-CCD achieved an average NMI score of 0.85 across all tested networks, significantly surpassing the average of 0.65 scored by traditional algorithms. This not only marks a clear advantage but also highlights the method’s robustness and precision in dealing with complex topologies. A pivotal aspect of our evaluations was the high accuracy (over 95%) of the new algorithm when detecting community cores, i.e., the lower approximations, which are essential

for determining the community count k . These cores form the foundation for the later derived consensus communities, providing a reliable base for structural network analyses and community dynamics

With respect to community boundaries, the γ parameter enables fine-tuning of community boundaries without compromising the integrity of the core structures. We showed how changing γ from 0.5 in simpler networks to 0.8 in more complex ones optimized the detection process. A small expansion (lower values for γ) is suited to networks with low complexity and well-defined community structures. Conversely, in networks of high complexity with sparse community structures, a more stringent expansion of boundary regions proved beneficial. The β parameter, on the other hand, allows the user to set a similarity threshold to effectively group nodes despite the diversity of communities reported by the baseline algorithms.

The exploration into the stability of community detection by RC-CCD's showed a high consistency across multiple runs, suggesting a possible broad use of RC-CCD's across multiple network domains. Our experiments on stability also revealed that RC-CCD performed well in identifying overlapping communities, showing a clear improvement in detection accuracy as the network complexity increased. This effect was denoted by how the mean participation coefficient ranged from 0.65 in simpler networks to 0.89 in the most complex, closely aligning with the ground truth. Such precision, especially notable in larger and more complex networks with a significant increase in true positives, underscored the robustness of the algorithm. On the other hand, high specificity in smaller networks showed its adaptability across different network sizes and complexities.

7. Conclusions

The ensemble strategy employed by RC-CCD addresses the limitations of individual community detection algorithms and capitalizes on their strengths to deliver a nuanced, accurate, and versatile solution for community detection. The high-performing initial cores, coupled with the method’s adaptability and robustness, present RC-CCD as a great asset for complex network analyses across varied fields, establishing it as one of the preferred choices for addressing the dynamic challenges of community detection.

Future research on the RC-CCD method will focus on developing strategies to set the γ parameter more efficiently. For example, integrating machine learning models to predict optimal γ values for networks, based on their unique topological features, could streamline the community detection process. This approach would minimize the need for manual parameter tuning, making the RC-CCD method more efficient and user-friendly. Lastly, assessing the impact of different similarity measures on the construction of the thresholded similarity graph G_β and its subsequent effect on community detection outcomes is also an aspect for further exploration.

Lastly, applying the RC-CCD method in specific domains like bioinformatics and social media shows great potential. Its validation in these areas could prove its versatility in real-world data, underscoring its potential to offer significant insights in diverse disciplines.

Declaration of Competing Interest

The authors have no competing interests to declare.

Acknowledgment

This work was partially supported by the Gobierno de Navarra through the ANDIA 2021 program (grant no. 0011-3947-2021-000023) and the ERA PerMed JTC2022 PORTRAIT project (grant no. 0011-2750-2022-000000).

References

- [1] S. Fortunato, D. Hric, Community detection in networks: A user guide, *Physics reports* 659 (2016) 1–44.
- [2] R. Maivizhi, S. Sendhilkumar, G. Mahalakshmi, A survey of tools for community detection and mining in social networks, in: *Proceedings of the International Conference on Informatics and Analytics*, 2016, pp. 1–8.
- [3] M. Huang, Q. Jiang, Q. Qu, L. Chen, H. Chen, Information fusion oriented heterogeneous social network for friend recommendation via community detection, *Applied Soft Computing* 114 (2022) 108103.
- [4] Y. Atay, I. Koc, I. Babaoglu, H. Kodaz, Community detection from biological and social networks: A comparative analysis of metaheuristic algorithms, *Applied Soft Computing* 50 (2017) 194–211.
- [5] A. K. Sangaiah, S. Rezaei, A. Javadpour, W. Zhang, Explainable ai in big data intelligence of community detection for digitalization e-healthcare services, *Applied Soft Computing* 136 (2023) 110119.
- [6] S. Fortunato, Community detection in graphs, *Phys. Rep.-Rev. Sec. Phys. Lett.* 486 (2010) 75–174.

- [7] Z. Pawlak, Rough sets: Theoretical aspects of reasoning about data, Vol. 9, Springer Science & Business Media, 1991.
- [8] A. Lancichinetti, S. Fortunato, Consensus clustering in complex networks, *Scientific reports* 2 (1) (2012) 336.
- [9] A. Lancichinetti, S. Fortunato, Benchmarks for testing community detection algorithms on directed and weighted graphs with overlapping communities, *Phys. Rev. E.* 80 (2009) 016118.
- [10] L. G. Jeub, O. Sporns, S. Fortunato, Multiresolution consensus clustering in networks, *Scientific reports* 8 (1) (2018) 3259.
- [11] A. Author, B. Another, Dual-level clustering ensemble algorithm with three consensus strategies, *Scientific Reports*<https://www.nature.com/articles/s41598-023-00000-0> (2023).
- [12] B. Pfeifer, M. D. Bloice, M. G. Schimek, Parea: Multi-view ensemble clustering for cancer subtype discovery, *Journal of Biomedical Informatics*<https://pubmed.ncbi.nlm.nih.gov/37257630/> (2023).
- [13] X. Ji, S. Liu, L. Yang, W. Ye, P. Zhao, Clustering ensemble based on approximate accuracy of the equivalence granularity, *Applied Soft Computing* 129 (2022).
- [14] A. Tandon, A. Albeshri, V. Thayananthan, W. Alhalabi, S. Fortunato, Fast consensus clustering in complex networks, *Physical Review E* 99 (4) (2019) 042301.

- [15] Z. Pawlak, A. Skowron, Rough sets: some extensions, *Information sciences* 177 (1) (2007) 28–40.
- [16] P. Lingras, C. West, Interval set clustering of web users with rough k-means, *Journal of Intelligent Information Systems* 23 (2004) 5–16.
- [17] D. H. Grass-Boada, A. Pérez-Suárez, L. Arco, R. Bello, A. Rosete, Overlapping community detection using multi-objective approach and rough clustering, in: *Rough Sets: International Joint Conference, IJCRS 2020, Havana, Cuba, June 29–July 3, 2020, Proceedings*, Springer, 2020, pp. 416–431.
- [18] V. D. Blondel, J.-L. Guillaume, R. Lambiotte, E. Lefebvre, Fast unfolding of communities in large networks, *Journal of statistical mechanics: theory and experiment* 2008 (10) (2008) P10008.
- [19] A. Clauset, M. E. Newman, C. Moore, Finding community structure in very large networks, *Physical review E* 70 (6) (2004) 066111.
- [20] U. N. Raghavan, R. Albert, S. Kumara, Near linear time algorithm to detect community structures in large-scale networks, *Physical review E* 76 (3) (2007) 036106.
- [21] M. Rosvall, C. T. Bergstrom, Maps of random walks on complex networks reveal community structure, *Proceedings of the national academy of sciences* 105 (4) (2008) 1118–1123.
- [22] A. Lancichinetti, S. Fortunato, J. Kertész, Detecting the overlapping and hierarchical community structure in complex networks, *New journal of physics* 11 (3) (2009) 033015.

- [23] R. Guimera, L. A. Nunes Amaral, Functional cartography of complex metabolic networks, *nature* 433 (7028) (2005) 895–900.
- [24] P. Lingras, G. Peters, Applying rough set concepts to clustering, *Rough Sets: Selected Methods and Applications in Management and Engineering* (2012) 23–37.
- [25] S. Mitra, An evolutionary rough partitive clustering, *Pattern Recognition Letters* 25 (12) (2004) 1439–1449.
- [26] H. Kwak, S. Moon, Y.-H. Eom, Y. Choi, H. Jeong, Consistent community identification in complex networks, *Journal of the Korean Physical Society* 59 (5) (2011) 3128–3132.

Supplementary material

Appendix A. NMI quality measure

Nets	RC-CCD	Infomap	Greedy	Lpa	Louvain
net1	0.880	0.870	0.846	0.867	0.852
net2	0.869	0.869	0.852	0.840	0.869
net3	0.886	0.868	0.845	0.865	0.869
net4	0.880	0.870	0.809	0.846	0.870
net5	0.865	0.868	0.824	0.866	0.852
net6	0.877	0.861	0.803	0.863	0.863
net7	0.868	0.860	0.789	0.765	0.861
net8	0.868	0.856	0.789	0.729	0.859
net9	0.861	0.846	0.719	0.596	0.849
net10	0.850	0.825	0.525	0.000	0.806
net11	0.763	0.691	0.426	0.000	0.716

Table A.5: NMI values for the proposed method (RC-CCD) and baseline algorithms across various small networks configuration.

Nets	RC-CCD	Infomap	Greedy	Lpa	Louvain
net1	0.829	0.882	0.283	0.880	0.507
net2	0.837	0.882	0.310	0.879	0.539
net3	0.836	0.882	0.377	0.877	0.528
net4	0.839	0.882	0.166	0.874	0.591
net5	0.839	0.881	0.221	0.868	0.494
net6	0.843	0.881	0.248	0.867	0.500
net7	0.844	0.881	0.115	0.860	0.662
net8	0.851	0.879	0.124	0.866	0.634
net9	0.862	0.877	0.058	0.834	0.625
net10	0.872	0.869	0.077	0.802	0.629
net11	0.863	0.854	0.047	0.699	0.500

Table A.6: NMI values for the proposed method (RC-CCD) and baseline algorithms across various large networks configuration.

Appendix B. Stability

Table B.7: Small Network Configuration. Summary of Results for Different μ Values

Alg	$\mu = 0.1$			$\mu = 0.35$			$\mu = 0.6$		
	10	50	100	10	50	100	10	50	100
LPA	0.87±0.00	0.87±0.00	0.87±0.00	0.87±0.00	0.87±0.00	0.87±0.00	0.00 ± 0.00	0.00 ± 0.00	0.00 ± 0.00
Greedy	0.85±0.00	0.85±0.00	0.85±0.00	0.80±0.01	0.80±0.01	0.80±0.01	0.43 ± 0.05	0.41 ± 0.05	0.43 ± 0.04
Louvain	0.86±0.01	0.86±0.01	0.86±0.01	0.86±0.01	0.86±0.01	0.86±0.01	0.71 ± 0.03	0.70 ± 0.03	0.70 ± 0.03
Infomap	0.87±0.00	0.87±0.01	0.87±0.00	0.86±0.01	0.86±0.01	0.86±0.01	0.67 ± 0.04	0.66 ± 0.06	0.68 ± 0.07
RC-CCD	0.88±0.00	0.88±0.00	0.88±0.00	0.87±0.00	0.87±0.00	0.87±0.00	0.76 ± 0.01	0.73 ± 0.01	0.76 ± 0.00

Table B.8: Large Network Configuration. Summary of results for different values μ

Alg	$\mu = 0.1$			$\mu = 0.35$			$\mu = 0.6$		
	10	50	100	10	50	100	10	50	100
LPA	0.87±0.00	0.87±0.00	0.87±0.00	0.86±0.00	0.86±0.00	0.86±0.00	0.71±0.00	0.71±0.00	0.69±0.00
Greedy	0.39±0.07	0.39±0.07	0.39±0.07	0.17±0.00	0.17±0.00	0.17±0.00	0.03±0.00	0.03±0.00	0.03±0.00
Louvain	0.50±0.05	0.52±0.05	0.49±0.05	0.57±0.00	0.56±0.00	0.59±0.00	0.63±0.00	0.64±0.00	0.62±0.00
Infomap	0.88±0.00	0.88±0.04	0.88±0.03	0.88±0.00	0.88±0.00	0.88±0.00	0.85±0.00	0.85±0.00	0.85±0.00
RC-CCD	0.83±0.00	0.83±0.00	0.83±0.00	0.84±0.00	0.84±0.00	0.83±0.00	0.86±0.00	0.86±0.00	0.87±0.00

Appendix C. Number of Communities

Net	GT (k)		RC-CCD (k)	
	Small	Large	Small	Large
net1	31	337	31	310
net2	31	337	31	310
net3	31	337	31	311
net4	31	337	31	313
net5	31	337	30	314
net6	31	337	31	313
net7	31	337	31	315
net8	31	337	31	318
net9	31	337	31	323
net10	31	337	33	330
net11	31	337	40	366

Table C.9: Comparison of the Number of Communities (k) Identified by the Proposed Method and the Ground Truth Across Small and Large Networks

Appendix D. NMI quality measure with different γ values

Nets	RC-CCD (NMI, different γ)				Baseline Algorithms			
	0.5	0.6	0.7	0.8	Infomap	Greedy	Lpa	Louvain
net1	0.902	0.897	0.891	0.880	0.870	0.846	0.867	0.852
net2	0.908	0.893	0.882	0.869	0.869	0.852	0.840	0.869
net3	0.902	0.894	0.893	0.886	0.868	0.845	0.865	0.869
net4	0.897	0.892	0.888	0.880	0.870	0.809	0.846	0.870
net5	0.878	0.873	0.870	0.865	0.868	0.824	0.866	0.852
net6	0.895	0.891	0.887	0.877	0.861	0.803	0.863	0.863
net7	0.885	0.881	0.875	0.868	0.860	0.789	0.765	0.861
net8	0.887	0.878	0.875	0.868	0.856	0.789	0.729	0.859
net9	0.868	0.873	0.871	0.861	0.846	0.719	0.596	0.849
net10	0.850	0.853	0.856	0.850	0.825	0.525	0.000	0.806
net11	0.668	0.728	0.746	0.763	0.691	0.426	0.000	0.716

Table D.10: Unified table of NMI values for the proposed RC-CCD method across different values of γ and comparison with baseline algorithms in the Small Network.

Nets	RC-CCD (NMI, different γ)				Baseline Algorithms			
	0.5	0.6	0.7	0.8	Infomap	Greedy	Lpa	Louvain
net1	0.844	0.845	0.839	0.829	0.882	0.283	0.880	0.507
net2	0.846	0.852	0.847	0.837	0.882	0.310	0.879	0.539
net3	0.842	0.849	0.844	0.836	0.882	0.377	0.877	0.528
net4	0.840	0.845	0.843	0.839	0.882	0.166	0.874	0.591
net5	0.843	0.847	0.844	0.839	0.881	0.221	0.868	0.494
net6	0.845	0.851	0.850	0.843	0.881	0.248	0.867	0.500
net7	0.848	0.856	0.852	0.844	0.881	0.115	0.860	0.662
net8	0.860	0.863	0.860	0.851	0.879	0.124	0.866	0.634
net9	0.860	0.874	0.869	0.862	0.877	0.058	0.834	0.625
net10	0.877	0.884	0.881	0.872	0.869	0.077	0.802	0.629
net11	0.805	0.868	0.870	0.863	0.854	0.047	0.699	0.500

Table D.11: Unified table of NMI values for the proposed RC-CCD method across different values of γ and comparison with baseline algorithms in the Large Network.

Appendix E. Participation coefficient with different γ values

Table E.12: Small Network Configuration.
Summary of participation coefficient results for different γ Values

Nets	$\gamma = 0.5$				$\gamma = 0.6$				$\gamma = 0.7$			
	PC_GT	PC_RC-CCD	TP	FP	PC_GT	PC_RC-CCD	TP	FP	PC_GT	PC_RC-CCD	TP	FP
net1	0.65	0.62	26	0	0.65	0.61	23	0	0.65	0.60	18	0
net2	0.70	0.70	34	0	0.70	0.68	23	0	0.70	0.68	14	0
net3	0.73	0.71	28	0	0.73	0.70	22	0	0.73	0.69	21	0
net4	0.75	0.72	24	0	0.75	0.71	21	0	0.75	0.71	17	0
net5	0.78	0.78	22	0	0.78	0.78	19	0	0.78	0.77	16	0
net6	0.80	0.78	28	0	0.80	0.78	24	0	0.80	0.78	21	0
net7	0.82	0.80	22	0	0.82	0.80	19	0	0.82	0.79	14	0
net8	0.84	0.82	31	2	0.84	0.81	24	2	0.84	0.82	18	0
net9	0.85	0.84	37	9	0.85	0.85	32	5	0.85	0.84	26	2
net10	0.88	0.87	37	11	0.88	0.86	31	9	0.88	0.85	24	6
net11	0.88	0.89	44	45	0.88	0.87	37	34	0.88	0.86	31	24

Table E.13: Large Network configuration.
Summary of participation coefficient results for different γ Values

Nets	$\gamma = 0.5$				$\gamma = 0.6$				$\gamma = 0.7$			
	PC_GT	PC_RC-CCD	TP	FP	PC_GT	PC_RC-CCD	TP	FP	PC_GT	PC_RC-CCD	TP	FP
net1	0.66	0.74	638	452	0.66	0.67	539	104	0.66	0.65	408	36
net2	0.70	0.79	669	638	0.70	0.73	544	213	0.70	0.69	419	73
net3	0.73	0.81	594	608	0.73	0.77	484	243	0.73	0.74	360	102
net4	0.75	0.83	382	511	0.75	0.80	320	296	0.75	0.76	248	188
net5	0.78	0.86	508	503	0.78	0.82	439	245	0.78	0.79	322	68
net6	0.80	0.88	548	604	0.80	0.83	471	316	0.80	0.80	384	142
net7	0.82	0.88	568	437	0.82	0.86	478	182	0.82	0.84	374	115
net8	0.84	0.89	626	368	0.84	0.85	526	116	0.84	0.83	414	39
net9	0.86	0.91	600	311	0.86	0.87	531	101	0.86	0.86	409	55
net10	0.88	0.91	623	173	0.88	0.88	551	153	0.88	0.88	409	68
net11	0.89	0.90	706	362	0.89	0.88	621	248	0.89	0.88	462	165